



Simulation of Nematic-Isotropic Phase Coexistence in Liquid Crystals under Shear

Guido Germano, Friederike Schmid

published in

NIC Symposium 2004, Proceedings,
Dietrich Wolf, Gernot Münster, Manfred Kremer (Editors),
John von Neumann Institute for Computing, Jülich,
NIC Series, Vol. **20**, ISBN 3-00-012372-5, pp. 311-320, 2003.

© 2003 by John von Neumann Institute for Computing

Permission to make digital or hard copies of portions of this work for personal or classroom use is granted provided that the copies are not made or distributed for profit or commercial advantage and that copies bear this notice and the full citation on the first page. To copy otherwise requires prior specific permission by the publisher mentioned above.

<http://www.fz-juelich.de/nic-series/volume20>

Simulation of Nematic-Isotropic Phase Coexistence in Liquid Crystals under Shear

Guido Germano^{1,2} and Friederike Schmid²

¹ Physical Chemistry
Philipps-University Marburg
35032 Marburg, Germany
E-mail: germano@staff.uni-marburg.de

² Theoretical Physics
University of Bielefeld
33501 Bielefeld, Germany
E-mail: schmid@physik.uni-bielefeld.de

Experiments and theories have shown that nematic fluids may adopt inhomogeneous steady states under shear flow. Here we reproduce and study such states by nonequilibrium molecular dynamics simulations of systems of soft repulsive ellipsoids. Different situations where a nematic phase coexists with a paranematic phase are examined. In geometries that impose constant stress on the whole system, we observe shear banding, i. e., separation into two phases with different local strain rates.

1 Introduction

According to common wisdom, matter at room temperature is either solid, liquid, or gaseous. However, this is not generally true. Certain materials — often “complex fluids” made of large, organic molecules — assume intermediate structures that combine properties of solids and liquids. For example, systems of anisotropic, cigar-shaped or rod-like molecules may exhibit a “nematic” phase, where the molecules have no translational order, but are still aligned along one preferential direction, the director¹. Because of its intermediate nature, this state of matter is called liquid-crystalline or a mesophase, and the molecules mesogens, or more specifically nematogens. Liquid-crystalline materials in which phase transitions between different states are mainly controlled by the temperature are classified as thermotropic liquid crystals. In solutions of nematogens, mesophase transitions may also be driven by the concentration of the nematogens. Such liquid crystals are called lyotropic. Liquid crystals have many technological applications especially in electro-optics; most well-known to the large public are flat displays.

Complex fluids often show unusual and interesting behavior under flow. Typical experimental setups designed to study such phenomena put the fluid into a state of steady shear flow by applying external shear stress. Prominent examples are the Couette cell, where fluids are confined between two concentric cylinders moving at different velocities, or the Poiseuille rheometer, where the fluid is forced to flow through a capillary tube. The streaming velocity field breaks the isotropy of space in the fluid, just as the director field breaks the symmetry in a nematic liquid crystal. When a nematic liquid crystal is sheared, one can thus anticipate interesting effects from the interplay of these two symmetry breaking fields.

Shear flow influences the order of liquid crystals at the molecular level, and therefore modifies macroscopic quantities like the viscosity (shear thinning or thickening). It may cause flow-controlled transitions between states that differ in their molecular alignment (shear banding). The behavior of the fluid can be described by a nonequilibrium phase diagram spanned by the density, the temperature and the strain rate or the shear stress. Such a phase diagram exhibits a nematic-isotropic coexistence region that is believed to culminate in a critical point at a high enough strain rate, in analogy with the equilibrium phase diagram of a liquid-gas system or of two immiscible fluids^{2,3}. In contrast to equilibrium phase diagrams, however, the nonequilibrium phase diagram is not uniquely defined, but depends on the details of the experimental setup.

In the coexistence region, the nematic and isotropic phases are separated by an interface that again breaks the isotropy of space and influences the molecular orientation in the nematic phase. This phenomenon is known as surface anchoring. All surfaces impose or at least favor one particular tilt angle between the director and the surface normal. Specifically, nematic/isotropic interfaces often favor planar anchoring, i. e., the molecules tend to lie flat on the surface.

Other important properties of fluid-fluid interfaces are the interfacial tension and the presence of small undulations, also called capillary waves. In addition to affecting the molecular order, shear introduces a new time scale into the fluid, $1/\dot{\gamma}$, where $\dot{\gamma}$ is the strain rate. As a consequence, long-lived fluctuations and large structural relaxation times with a lifetime longer than $1/\dot{\gamma}$ should be destroyed or at least reduced in sheared systems. One would thus expect that shear affects the long-wavelength capillary waves, which are very long-lived, and possibly modifies the closely related effective interfacial tension.

Nematic fluids in shear flow have been studied for the last 25 years experimentally, theoretically, and by computer simulation. Literature overviews can be found in Refs. 2 and 3. Experiments include rheological, optical (e.g. anomalous light scattering) and spectroscopic (e.g. nuclear magnetic resonance) techniques. Theoretical studies were based on generalizations of the Navier-Stokes equations, i. e., coupled hydrodynamic equations of motion for the nematic order tensor \mathbf{Q} and the streaming velocity of the fluid \mathbf{v}_s , that depend on the strain rate $\dot{\gamma}$ (or its generalisation, the velocity gradient tensor), the density ρ , the temperature T , and rotational and shear viscosities η_r and η_s . Such equations have been used to calculate nonequilibrium phase diagrams for thermotropic² and lyotropic³ liquid crystals in various experimental geometries.

In the project presented here, we have performed a computer simulation of such a system. In contrast to the theory mentioned above, that describes the system as a continuum, we adopt a particle-based approach and study a system of ellipsoids in shear flow. To our knowledge, this is the first multiphase nonequilibrium simulation of a liquid crystal: previous simulations we are aware of have been aimed at computing viscosities and other transport coefficients of homogeneous mesophases. Simulations of inhomogeneous liquid crystals under shear are particularly challenging, since they require non-standard software and are computationally very expensive.

Our paper is organized as follows. In the next section, we define the model and discuss some technical details. Results are presented in section 3. Finally, we summarize and conclude in section 4.

2 Model and Simulation Method

We model molecules in a classical mechanics framework as soft repulsive ellipsoids with a length to width ratio of 15. This particular choice permits a direct comparison with previous equilibrium studies of the surface tension⁴ and capillary wave fluctuations⁵ of the nematic-isotropic interface in the same system. Each molecule is fully determined by the position of its center of mass \mathbf{r} and by the unit vector $\hat{\mathbf{u}}$ that identifies its long axis. The intermolecular potential is

$$U = \begin{cases} \sum_{i < j} 4\epsilon_0(s_{ij}^{-12} - s_{ij}^{-6}) + \epsilon_0, & s_{ij} < 2^{1/6} \\ 0, & \text{otherwise} \end{cases}, \quad (1)$$

where $s_{ij} = (r_{ij} - \sigma(\hat{\mathbf{r}}_{ij}, \hat{\mathbf{u}}_i, \hat{\mathbf{u}}_j) + \sigma_0)/\sigma_0$ is a scaled and shifted distance with σ approximating⁶ the contact distance of two ellipsoids. All data in this paper are given in reduced units defined by the energy and length parameters ϵ_0 and σ_0 , the particle's mass and the Boltzmann constant. We perform a Molecular Dynamics (MD) simulation, i. e., the molecular positions \mathbf{r}_i and the orientations $\hat{\mathbf{u}}_i$ are propagated according to Newton's equations of motion, more specifically using the symplectic integration algorithm RATTLE⁷.

As usually done in this type of simulations, the molecules are contained in a cuboidal box with periodic boundary conditions. This means that the box is surrounded by mirror images of itself so as to avoid surface effects. Shear flow can be enforced by moving the boundaries at constant speed⁸. In other words, the mirror images along the y axis are shifted at each time step with respect to the box by an amount $\dot{\gamma}L_y\Delta t$, where L_y is the length of the box along the y direction. The energy constantly pumped into the system by this means must be dissipated at the same rate it comes in so that a steady nonequilibrium state can be reached. We achieved this by coupling the molecular velocities to a Nosé-Hoover extended Lagrangian thermostat⁹. We took care that it acts only on the disordered, thermal part of the velocities, i. e., the velocities minus the streaming velocity of the fluid. It is important that the thermostat is unbiased by the velocity profile when the latter is not uniform due to the presence of an interface, as in our case.

Given the intermolecular potential function and the density, temperature and strain rate parameters, MD allows to measure the streaming velocity field, the order tensor, the stress tensor, and the viscosities. The order tensor is given by

$$\mathbf{Q} = \frac{1}{N} \sum_{i=1}^N \left(\frac{3}{2} \hat{\mathbf{u}}_i \otimes \hat{\mathbf{u}}_i - \frac{1}{2} \mathbf{I} \right), \quad (2)$$

where \mathbf{I} is the 3×3 unity matrix. The nematic order parameter P_2 is the highest eigenvalue of \mathbf{Q} , and the director $\hat{\mathbf{n}}$ is the eigenvector corresponding to P_2 . The stress tensor (equal to the negative pressure tensor \mathbf{P}) is given by

$$\boldsymbol{\sigma} = -\mathbf{P} = -\frac{1}{V} \left(\sum_{i=1}^N m_i \mathbf{v}_i \otimes \mathbf{v}_i + \sum_{i < j=1}^N \mathbf{r}_{ij} \otimes \mathbf{f}_{ij} \right). \quad (3)$$

The shear viscosity is defined by

$$\eta_s = \frac{\sigma_{xy}}{\dot{\gamma}}, \quad \text{where} \quad \dot{\gamma} = \frac{\partial v_x}{\partial r_y} \quad (4)$$

is the locally observed strain rate, while $\Delta v_x/\Delta r_y = \Delta v_x/L_y$ is the globally imposed strain rate.

At this point, a few remarks regarding the choice of the model are in order. On principle, one could of course implement a more realistic molecular potential, that contains intramolecular degrees of freedom or even atomic detail. This would permit quantitative comparisons with experiments. Unfortunately, it would also increase the already high computational cost to a currently unbearable extent. Therefore, we have restricted ourselves to studying a simple, computationally cheap model system. Comparisons are thus mainly with theories. This reflects the peculiarity of simulations, that have an intermediate position between experiments and theories.

In usual bulk simulations of ordinary liquids with periodic boundary conditions, good results can be obtained with systems of only a few hundred molecules. Mesophases require larger system sizes, due to the long range ordering and the presence of collective properties. Nevertheless, thousand molecules will often be sufficient. In order to observe a phase separation, however, one must use elongated simulation boxes that contain several thousand molecules, or cubic boxes with even more particles. The smallest systems studied in this work contained 7200 particles in a box with side ratios 1:8:1. If one wishes to study interface properties like capillary wave fluctuations, the cross-section of the interface must be very large, and the necessary number of particles increases by yet another order of magnitude, totalling about 10^5 . Our largest system contained 115200 particles. It was initially set up by replicating the system with $N = 7200$ particles four times along the x axis and four times along the z axis. Runs of up to a few million MD time steps were necessary to equilibrate the system and gather enough statistics.

The need for a massively parallel computer is thus evident. Our MD program exploits parallelism by domain decomposition, i. e., it splits the simulation box into smaller domains that are each processed by a different processor. Only nearest neighbor domains exchange particles with each other. The speed-up of the program has been tested on the Cray T3E. It scales well on up to as many nodes as were available (512), though for production only one quarter (128) of the maximum was used. The communication paradigm is MPI.

3 Results

Following a common convention, we label the flow (or velocity) axis x , the flow (or velocity) gradient axis y , and the third axis, called vorticity axis, z (see Fig. 1). In equilibrium (i. e., with normal periodic boundary conditions), a biphasic system consists of a slab of one phase, that is sandwiched between two regions of the other phase. The slab is inevitably perpendicular to one of the box sides, usually the longest one. In other words, there are always two parallel interfaces, that lie either in the xy plane, the xz plane, or the yz plane. When shear is applied (i. e., with moving boundary conditions), only the two first cases are stable.

When the interface lies in the xz plane, the two phases are subject to the same common shear stress σ_{xy} , but may have different strain rates $\dot{\gamma}$; when the interface lies in the xy plane, the two phases have the same strain rate, but may experience different shear stresses. In a Couette rheometer, where the vorticity axis corresponds to the spinning axis of the cylinders, the two phases form concentric rings in the common stress geometry and annular

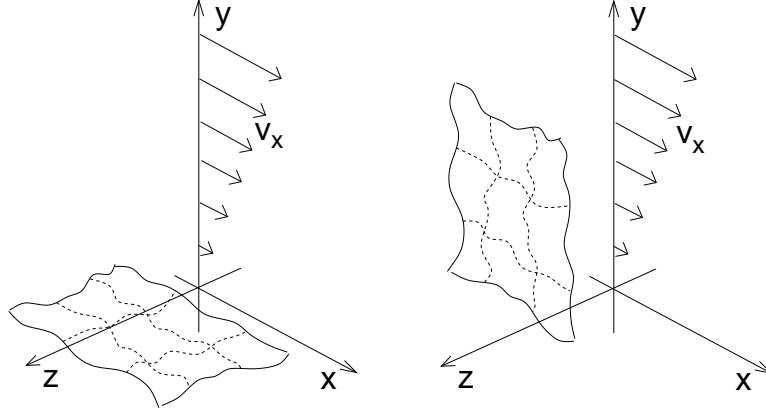


Figure 1. Reference system defined by the velocity profile \mathbf{v} and the two possible positions of an interface: common stress (left) and common strain (right) geometries.

bands in the common strain geometry.

In a system of soft ellipsoids such as the one considered here, the interface aligns the director in the direction parallel to the surface⁴ (planar anchoring). Thus the nematic director $\hat{\mathbf{n}}$ lies on the interface plane. At common stress, two different locally stable arrangements of the director with respect to the flow direction x are predicted by theory and observed in experiments, depending on how the system was prepared: parallel (flow-aligning) and perpendicular (log-rolling). At common strain, only the flow-aligning case is stable.

We have simulated a system with $N = 115200$ particles in the nematic-isotropic coexistence region in the common stress, flow-aligning geometry. The average density was $\rho = 0.017$, the temperature $T = 1.0$, and the strain rates $\dot{\gamma}$ ranged from 10^{-5} to 10^{-1} . In all cases, the initial configuration was an equilibrated zero-shear system containing two interfaces. A snapshot of the $\dot{\gamma} = 10^{-3}$ system is shown in Fig. 2.

At low strain rates, the density and the order parameter take two clearly distinct values in the different phases (Fig. 3). The order parameter in the isotropic phase is almost zero. In fact, the remaining small value does not differ substantially from that calculated at zero shear in the isotropic phase. Nevertheless, it should be noted that flow is bound to induce a tiny amount of order in the disordered phase, since it breaks the isotropy of space. Strictly speaking, the “isotropic” phase should be more properly called paranematic.

At higher strain rates ($\dot{\gamma} = 10^{-2}$ and 10^{-1}), the two phases merge and the interfaces disappear. This can be seen by monitoring the order parameter and the density of the system along the y axis. At the highest strain rate $\dot{\gamma} = 10^{-1}$, the order parameter profile shows quite pronounced differences in the initial configuration, that level off rapidly within a few tens of thousand MD steps (Fig. 4). The density profile follows more slowly. A similar process takes place at $\dot{\gamma} = 10^{-2}$, though on a longer time scale.

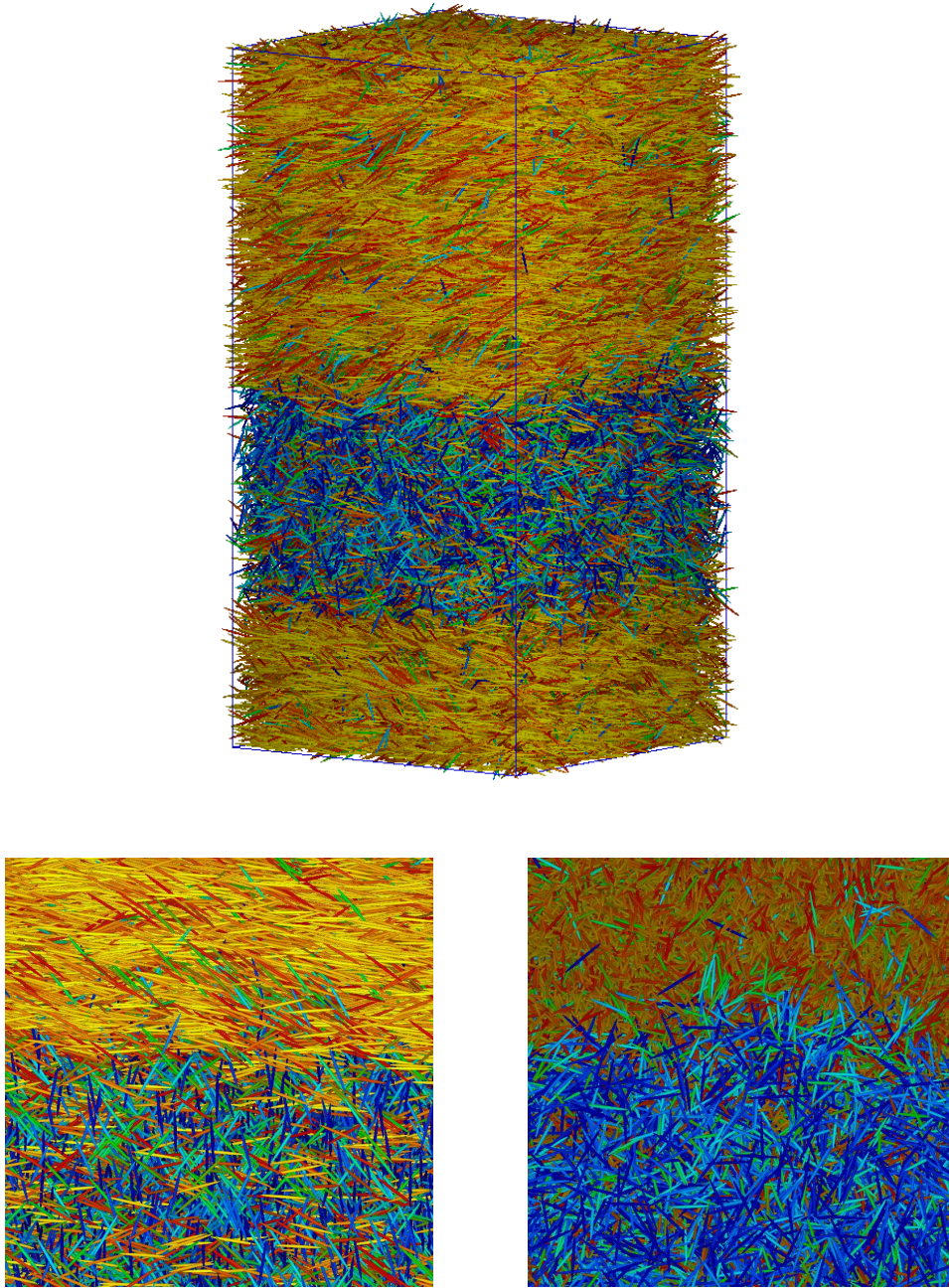


Figure 2. **Top:** Snapshot of a common stress, flow-aligning system with $\dot{\gamma} = 10^{-3}$ (115200 particles). The reference system and interface geometry are as in the left of Fig. 1. Molecules are coloured according to their orientation in order to show the difference between the two differently ordered phases. **Bottom left:** Detail of the interface region seen from the vorticity (z) axis. The molecules in the upper, nematic phase are clearly aligned from left to right along the flow axis (x). **Bottom right:** Detail of the interface region seen from the flow (x) axis. Though the lower phase shows some amount of flow-induced order, the view along x is more similar to the view along z than for the upper phase.

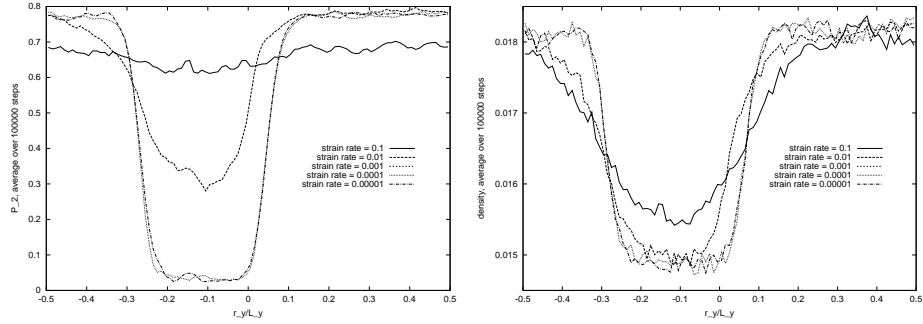


Figure 3. Order parameter (left) and density (right) profiles for common stress, flow-aligning systems at different strain rates, after more than 100,000 MD time steps. The high order, high density region corresponds to a nematic phase, the other to an isotropic (or paranematic) phase. At high strain rates, the two phases merge; the still incomplete merging process is faster for the order parameter than the density, and for the higher strain rate.

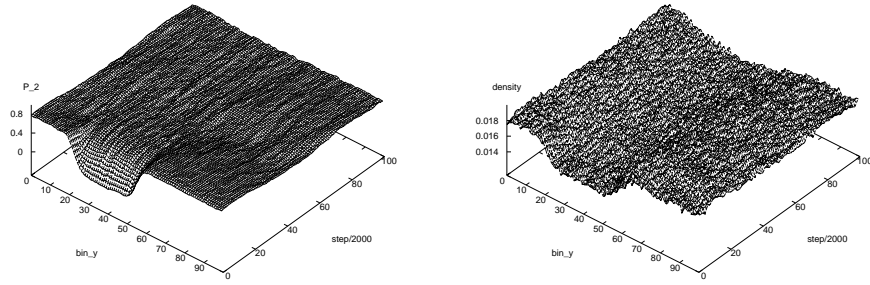


Figure 4. Approach to equilibrium of the order parameter (left) and density (right) profiles in the common stress, flow-aligning system with $\dot{\gamma} = 0.1$. The order parameter reacts faster than the density to an applied strain.

Having found that the interfaces are unstable at strain rates of $\dot{\gamma} = 10^{-2}$ and beyond, we chose to focus on the strain rate $\dot{\gamma} = 10^{-3}$ in most further studies, and accumulated about 2 million MD steps in the common stress, flow-aligning geometry. We set up another system in the common stress, log-rolling geometry by rotating the initial configuration of the common stress, flow-aligning case by 90° around the y axis, such that the director of the nematic phase was normal to the flow axis. We ran this system for 1.7 million steps, and so far it has remained stable. Order parameter and density profiles are identical with the flow-aligning case, see Fig. 5. A third system of again $N = 115200$ particles was set up by rotating the same initial configuration by 90° around the x axis, such that it can be sheared at common strain. The interface lies in the xy plane, as shown in the right part of Fig. 1. We have not yet accumulated enough data on this system to present them here.

At common stress, nonequilibrium interfaces exhibit another important feature: the local strain rate in the two coexisting phases is different. This is demonstrated in Fig. 6: in the more ordered phase the slope of the velocity profile is higher, i. e. the shear viscosity is lower. Intuitively, one can argue that the more aligned the particles are, the less resistance

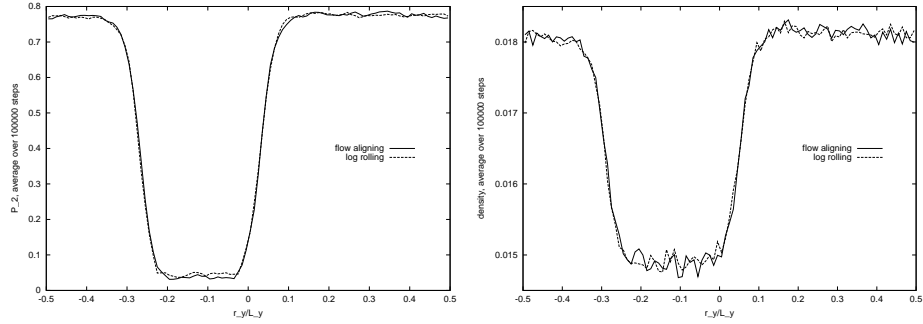


Figure 5. Common stress profiles for the flow-aligning and log-rolling systems with $\dot{\gamma} = 0.001$: order parameter (left) and density (right).

they oppose to the flow. This is observed both for alignment parallel and perpendicular to the flow direction, though the phenomenon is slightly more enhanced in the flow-aligning case, as one might expect. Shearing induces order, and order reduces the shear viscosity; the system is said to “shear thin”. This is consistent with the experience that systems with Lennard-Jones and similar potentials tend to shear thin: the soft ellipsoid potential is an anisotropic variant of the purely repulsive Lennard-Jones potential. However, there are also systems that shear thicken.

In addition to these studies, we have also attempted to assess more systematically the stability of the interface at different strain rates. To this end, we have simulated smaller systems of $N = 7200$ particles in a simulation box with side ratios 1:8:1 at strain rates between 0.002 and 0.009 in increments of 0.001, for all three geometries. We found that the interface remains stable up to an average strain rate of 0.006. Interestingly, the densities of the two coexisting phases do almost not depend on the strain rate at all. Beyond $\dot{\gamma} = 0.006$, the coexistence region disappears abruptly and the two phases merge in one. Combining the results from linear fits to the density and the velocity profiles, one can construct nonequilibrium phase diagrams. The result for the flow-aligning geometry is shown in Fig. 7.

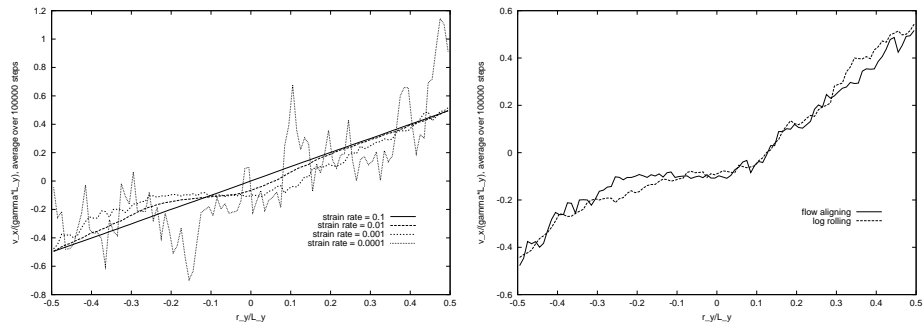


Figure 6. Shear banding in common stress velocity profiles: flow-aligning, several strain rates $\dot{\gamma}$ (left); flow-aligning and log-rolling, $\dot{\gamma} = 0.001$ (right).

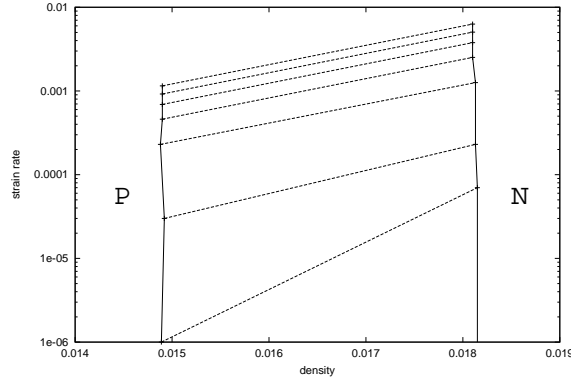


Figure 7. Phase diagram section at $T = 1$ of the common stress, flow-aligning system. P = paranematic region, N = nematic region. The sloped straight “tie” lines connect coexisting phases.

4 Conclusions and Outlook

To our knowledge, we have performed the first molecular simulation study of nonequilibrium interfaces under shear flow in liquid crystals. We have reproduced the inhomogeneous steady states predicted theoretically by Olmsted et al^{2,3}, for the three relevant geometries: flow-aligning nematic-paranematic in the constant stress and the constant strain geometries, and flow-aligning nematic-paranematic in the constant stress geometry. Most notably, we observed shear banding in the common stress geometry: at certain densities, the system separates into two phases, that respond with different strain rates to the same constant applied stress. The more ordered phase has the higher strain rate, i. e., we observe shear thinning upon ordering. Interestingly, this shear thinning occurs for both the flow-aligning and the log-rolling geometry, i. e., regardless of whether the director in the more ordered phase points along the flow or not. However, the effect seems to be a little stronger in the flow-aligning case, where the director and the velocity field are parallel. Furthermore, we have constructed a phase diagram of the coexistence region in the common stress geometry by analyzing the discontinuities of the order parameter, the density, and the local strain rate as a function of the total imposed strain.

In the present paper, we have presented only some preliminary results gathered in this study. A more detailed analysis will be presented elsewhere¹⁰, along with the results for the common strain geometry. In particular, we will study the biaxiality, the stress tensor, the interface tension, and the capillary wave fluctuations mentioned in the introduction. In future studies, attention shall also be given to transient phenomena such as the destruction of the interfaces at high strain rates, the flow-alignment of the director when shear is applied to a system oriented in a direction different from the direction of the flow, and the destruction of an interface that is set up in an unstable geometry, with the flow pointing normal to the interface. Due to the short-lived nature of these time-dependent phenomena, however, it is likely that it will not be possible to perform a quantitative analysis on the same level as for the steady states.

Acknowledgments

We are grateful to Peter D. Olmsted for a useful conversation, and to Radovan Bast for running many $N = 7200$ systems within an undergraduate physical chemistry project. The parallel molecular dynamics program GBMEGA was originally developed by the UK EPSRC Complex Fluid Consortium and kindly made available by Michael P. Allen. Thanks are due also to the DFG for funding, and to the NIC in Jülich for generous allocation of computing time.

References

1. P.-G. de Gennes, J. Prost, *The Physics of Liquid Crystals*, (Oxford University Press, 1995).
2. P. D. Olmsted, P. M. Goldbart, Phys. Rev. A **46**, 4966–4993 (1992).
3. P. D. Olmsted, C.-Y. D. Lu, Phys. Rev. E **60**, 4397–4415 (1999).
4. A. J. McDonald, M. P. Allen, F. Schmid, Phys. Rev. E. **63**, 010701-1–4 (2000).
5. N. Akino, F. Schmid, M. P. Allen, Phys. Rev. E **63**, 041706-1–6 (2001).
6. B. J. Berne, P. Pechukas, J. Chem. Phys **56**, 4213–4216 (1972).
7. M. P. Allen, D. J. Tildesley, *Computer Simulation of Liquids*, (Oxford University Press, Oxford, 1989).
8. D. J. Evans, G. P. Morriss, *Statistical Mechanics of Nonequilibrium Fluids*, (Academic Press, San Diego, 1990).
9. D. Frenkel, B. Smit, *Understanding Molecular Simulation*, (Academic Press, San Diego, 1996).
10. G. Germano, F. Schmid, manuscript in preparation (2003).